A novel class of two-dimensional chaotic maps with infinitely many coexisting attractors*

Li-Ping Zhang(张丽萍)[1,2]，Yang Liu(刘洋)[3]，Zhou-Chao Wei(魏周超)[4], Hai-Bo Jiang(姜海波)[2†] and Qin-Sheng Bi(毕勤胜)[1]

[1]Faculty of Civil Engineering and Mechanics, Jiangsu University, Zhenjiang 212013, China

[2]School of Mathematics and Statistics, Yancheng Teachers University, Yancheng 224002, China

[3]College of Engineering, Mathematics and Physical Sciences, University of Exeter, Exeter EX4 4QF, UK

[4]School of Mathematics and Physics, China University of Geosciences, Wuhan 430074, China

Abstract

This paper studies a novel class of two-dimensional maps with infinitely many coexisting attractors. Firstly, the mathematical model of these maps is formulated by introducing a sinusoidal function. The existence and the stabilities of the fixed points in the model are studied indicating that they are infinitely many and all unstable. In particular, a computer searching program is employed to explore the chaotic attractors in these maps, and a simple map is exemplified to show their complex dynamics. Interestingly, this map contains infinitely many coexisting attractors which has been rarely reported in the past literature. Further studies of these coexisting attractors are carried out by investigating their time histories, phase trajectories, basins of attraction, Lyapunov exponents spectrum and Lyapunov (Kaplan-Yorke) dimension. Bifurcation analysis reveals that the map has periodic and chaotic solutions, and more importantly, exhibits extreme multi-stability.

Keywords: Two-dimensional map, infinitely many coexisting attractors, extreme multi-stability, chaotic attractor.

PACS: 05.45.Ac, 05.45.Pq

1. Introduction

The phenomenon that a dynamical system displays more than one attractor under different initial conditions is called multi-stability. Multi-stability has been extensively investigated in the literature since it was found in many areas, such as physics, chemistry, biology and economics, see e.g. [1–5]. Some multi-stability is undesirable

---

†Corresponding author. E-mail:yctcjhb@126.com

since system can be perturbed to an undesired attractor in the presence of noise. So control of multi-stability has received considerable attention[6,7]. Liu and Páez Chávez[6] studied the control of coexisting attractors in an impacting system based on linear augmentation. On the other hand, multi-stability can be used to obtain the desired performance of a system without changing its parameters[4,8]. For example, Liu and Páez Chávez[8] investigated the control of multistability in a vibro-impact capsule system driven by a harmonic excitation using numerical continuation. The motion of the capsule system can be controlled by switching between its two stable coexisting attractors via a proper selection of their initial conditions. Very recently, hidden coexisting attractors, whose's basins of attraction are not connected with unstable equilibria, have been explored intensively, see g.g. [9,10].

There are one special type of multi-stability, namely, extreme multi-stability which means that the number of coexisting attractors tends to infinite. In [11–14], infinitely many coexisting attractors belong to extreme multi-stability have been explored extensively by using different types of coupling. In [15,16], the authors presented a method for designing an appropriate coupling scheme for two dynamical systems in order to realize extreme multi-stability. Then extreme multi-stability was first observed in experiment[17]. Apart from coupling method, there are several other methods to generate extreme multi-stability. Some researchers introduced one[18–24], two[25–28] and multiple[29] ideal memristors into nonlinear systems to show infinitely many coexisting attractors. For example, in [27], a novel five-dimensional two-memristor-based dynamical system was constructed by introducing two memristors with cosine memductance and extreme multi-stability was obtained. Other researchers constructed new chaotic systems with extreme multi-stability using proper nonlinear functions[30–36] or state feedback controller[37,38]. For example, in [30,31], the offset boosting method was developed to construct a self-reproducing system from a unique class of variable-boostable systems, and then extreme multi-stability was obtained. In [32], infinitely many strange attractors on a 3-D spatial lattice was obtained in a new dynamical system based on Thomas' system by using the disturbed offset boosting of sinusoidal functions with different spatial periods. Jafari et al.[35] constructed a new five-dimensional chaotic system displaying hidden attractors and extreme multi-stability. In [37], a novel 4D chaotic system presenting extreme multi-stability was derived by using a simple state feedback controller in a three-dimensional chaotic system.

Since nonlinear maps have broad applications in different disciplines including economics, biology, and engineering, smooth and non-smooth maps have been studied extensively in the literature[5,39–53]. Jiang et al.[40,41] explored coexisting hidden chaotic attractors in a class of two-dimensional and three-dimensional maps. Then Jiang et al.[42] studied multi-stability in a class of two-dimensional chaotic maps with closed curve fixed points by showing three cases of coexisting attractors. In [44–46], the authors investigated complex chaotic dynamics of several fractional-order chaotic maps, and in [47] fractional-order chaotic maps were used for image encryption. In [48,49], a sine chaotification model (SCM) was introduced to enhance the complexity of one-dimensional and two-dimensional chaotic maps, respectively. However, it is rare to observe extreme multi-stability in nonlinear maps. In [50], infinite coexistence of a piecewise-linear continuous map was proved directly by explicitly computing periodic solutions in the infinite sequence. In [51], an equivalence between infinitely many asymptotically stable periodic solutions of n-dimensional piecewise-linear continuous maps and their subsumed homoclinic connections was established.

This paper aims to explore some simple chaotic maps with infinitely many coexisting attractors, whose fixed

points are infinite and unstable, by performing an exhaustive computer search[52,53]. The main work of this paper is as follows: (1) A novel class of two-dimensional chaotic maps with infinitely many coexisting attractors is developed; (2) The chaotic attractors is numerically analyzed by using basin of attractions, the Lyapunov exponent spectrum (Les) and the Kaplan-Yorke dimension; (3) Bifurcation analysis of the map is conducted to show different types of infinitely many coexisting attractors, including infinitely many coexisting periodic solutions and infinitely many coexisting chaotic solutions. The rest of this paper is organized as follows. In Section 2, the mathematical model of this class of two-dimensional maps is introduced, and the existence and the stability of their fixed points are studied. In Section 3, infinitely many coexisting attractors and bifurcation phenomena in the maps are shown. Finally, concluding remarks are drawn in Section 4.

2. System model

Lai et al.[36] obtained an extremely simple chaotic system with infinitely many coexisting attractors by introducing a sinusoidal function into the Sprott B system. Following the idea of Lai et al.[36], we introduce a sinusoidal function into a class of two-dimensional maps to generate infinitely many coexisting attractors. By using a computer searching program [52,53], we studied a novel class of two-dimensional maps written by

$$
\begin{cases}
x_{k+1} = x_k + ax_k \sin(y_k), \\
y_{k+1} = y_k + bx_k + c,
\end{cases}
\tag{1}
$$

where x_k and y_k $(k = 0, 1, 2, \cdots)$ are system states at step k, $a \neq 0$, $b \neq 0$ and $c \neq 0$ are system parameters. The map (1) is periodic with regard to variable y, and the period is 2π. So the map (1) has a translational symmetry, i.e., $S(x, y + 2m\pi) = S(x, y)$, where $S(x, y) = (ax \sin(y), bx + c)$, $m = 0, \pm 1, \pm 2, \cdots$.

The fixed points (x^*, y^*) of the map (1) must satisfy the following conditions

$$
\begin{cases}
x^* = x^* + ax^* \sin(y^*), \\
y^* = y^* + bx^* + c.
\end{cases}
\tag{2}
$$

By solving Eq. (2), we have $(x^*, y^*) = (-c/b, m\pi)$, where $m = 0, \pm 1, \pm 2, \cdots$, which are infinite fixed points.

The Jacobian matrix of the map (1) at the fixed points (x^*, y^*) can be written as

$$
J = \begin{bmatrix} 1 & -ac\cos(y^*)/b \\ b & 1 \end{bmatrix},
\tag{3}
$$

The characteristic equation of the Jacobian matrix can be calculated using

$$
\det(\lambda I - J) = \lambda^2 - \mathrm{tr}(J)\lambda + \det(J) = 0,
\tag{4}
$$

where $\det(J) = 1 + ac\cos(y^*)$ and $\mathrm{tr}(J) = 2$ represent the determinant of the Jacobian matrix and the trace of the Jacobian matrix, respectively. Eigenvalues of J, λ_1 and λ_2 are called multipliers of the fixed point. The fixed point is stable if the roots of the characteristic equation, λ_1 and λ_2 satisfy that $|\lambda_{1,2}| < 1$, where $|\cdot|$ denotes the modulus of a complex number.

The map (1) can generate many different strange chaotic attractors and several simple chaotic maps were found, e.g. $(a, b, c) = (\pm 2.7, \pm 1, \pm 0.1)$. In this paper, one simple chaotic map with infinitely many coexisting

attractors was chosen to show the complex dynamics of this class of maps firstly. When $a = 2.7$, $b = 1$ and $c = 0.1$, the map (1) becomes

$$\begin{cases} x_{k+1} = x_k + 2.7 x_k \sin(y_k), \\ y_{k+1} = y_k + x_k + 0.1. \end{cases} \qquad (5)$$

The fixed points (x^*, y^*) of the map (5) are $(x^*, y^*) = (-0.1, \pm m\pi)$, where $m = 0, 1, 2, \cdots$. The Jacobian matrix of the map (5) at the fixed points $(-0.1, \pm 2m\pi)$ are $J_1 = \begin{bmatrix} 1 & -0.27 \\ 1 & 1 \end{bmatrix}$. The eigenvalues of J_1 are $\lambda_1^1 = 1.0000 + 0.5196i$, $\lambda_2^1 = 1.0000 - 0.5196i$, where i is the imaginary unit satisfying $i^2 = -1$. The Jacobian matrix of the map (5) at the fixed points $(-0.1, \pm(2m+1)\pi)$ are $J_2 = \begin{bmatrix} 1 & 0.27 \\ 1 & 1 \end{bmatrix}$. The eigenvalues of J_2 are $\lambda_1^2 = 1.5196$, $\lambda_2^2 = 0.4804$, respectively. Since $|\lambda_1^1| = |\lambda_1^2| = 1.1269 > 1$ and $|\lambda_1^2| = 1.5196 > 1$, all the fixed points are unstable.
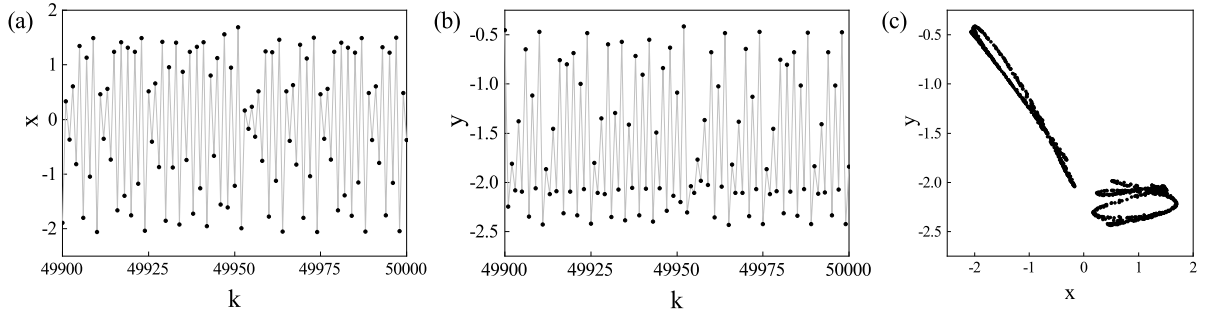

Fig. 1. Time histories of (a) x, (b) y, and (c) phase portrait of the chaotic attractor of the map (5) calculated by using the initial value $(1, -3)$.

When the initial value is chosen at $(1, -3)$, the map (5) displays chaotic attractor as shown in Fig.1. Fig.1 (a) and (b) show x and y of the chaotic attractor as a function of the step k, respectively. Fig.1 (c) presents the phase portrait of the chaotic attractor which is a two-piece chaotic attractor. The Lyapunov exponent spectrum (LEs) and the Kaplan-Yorke dimension (Dky) of the chaotic attractors were computed by using the Wolf methods given in [53,54]. Based on our simulation, Lyapunov exponent spectrum (LEs) of the chaotic attractor are $0.2711, -0.3602$, and its Lyapunov (Kaplan-Yorke) dimension (Dky) of the chaotic attractor is 1.7526.

3. Dynamical behaviors of the chaotic map with infinitely many coexisting attractors

3.1. Infinitely many coexisting attractors

Fig. 2 shows the phase portraits of coexisting chaotic attractors in the region $\{(x, y) | x \in [-2.5, 2.5], y \in [-30, 30]\}$. The coexisting chaotic attractors (i)-(ix) were calculated by using the initial conditions $(1, -28)$, $(1, -22)$, $(1, -16)$, $(1, -9)$, $(1, -3)$, $(1, 3)$, $(1, 10)$, $(1, 16)$ and $(1, 22)$, respectively. To see them clearly, theses chaotic attractors are presented in additional windows using different colors at an appropriate axis. From Fig. 2, these chaotic attractors are two-piece chaotic attractors in a similar structure. To investigate these attractors

in detail, basins of attraction of this map are plotted in Fig. 3, where the coexisting chaotic attractors are marked in black dots, and their basins are indicated by different colours. It can be seen from the figure that, the map (5) has fractal basin structure, and the basins of these coexisting chaotic attractors are similar but not uniform. It should be noted that, the initial values which lead the trajectory of the map to the region $\{(x,y)||x|+|y| > 100\}$ are considered as unbounded basins, and they are shown in cyan in the figure.
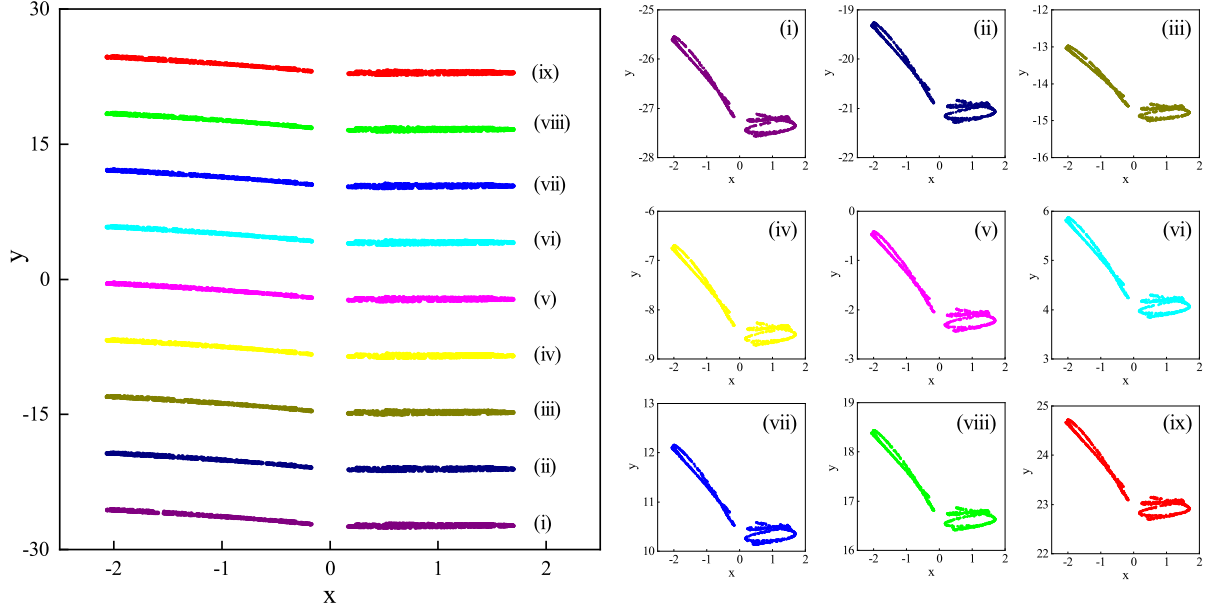

Fig. 2. (Colour online) Phase portraits of coexisting chaotic attractors of the map (5) calculated for $x(0) = 1$ and (i) $y(0) = -28$, (ii) $y(0) = -22$, (iii) $y(0) = -16$, (iv) $y(0) = -9$, (v) $y(0) = -3$, (vi) $y(0) = 3$, (vii) $y(0) = 10$, (viii) $y(0) = 16$, (ix) $y(0) = 22$, respectively.

By the translational symmetry, the map (5) can generate infinitely many coexisting attractors, which were rarely studied in the literature before. In [23], extreme multi-stability was classified as homogenous and heterogeneous extreme multi-stability according to the different characteristics of coexisting attractors. When a system generates the infinitely coexisting attractors having the same shape but different amplitudes, frequencies or positions, the system has homogenous extreme multi-stability. While a system has infinitely many different types of coexisting attractors, the system has heterogeneous extreme multi-stability. Since the coexisting chaotic attractors of the map (5) have the same shape but at different positions, the map has the translational symmetry displaying homogenous extreme multi-stability.

3.2. Bifurcation analysis

In order to show the complex dynamics of the chaotic map (1) with infinitely many coexisting attractors, bifurcation and Lyapunov exponent spectrum diagrams of the map are plotted in Fig. 4 by using a as a branching parameter and fixing (b, c) as $(1, 0.1)$, where the initial value was chosen as $(1, -3)$, and the final state values at the end of each iteration of the parameter serves as the initial state for the next iteration. Attractors denoted by black dots are shown in Fig. 4 (a), and representative phase portraits of the map with different parameter a are shown in additional windows. The largest Lyapunov exponent (Le1), the smallest Lyapunov exponent (Le2) and the Lyapunov (Kaplan-Yorke) dimension (Dky) are indicated by red, blue and black lines in Fig. 4
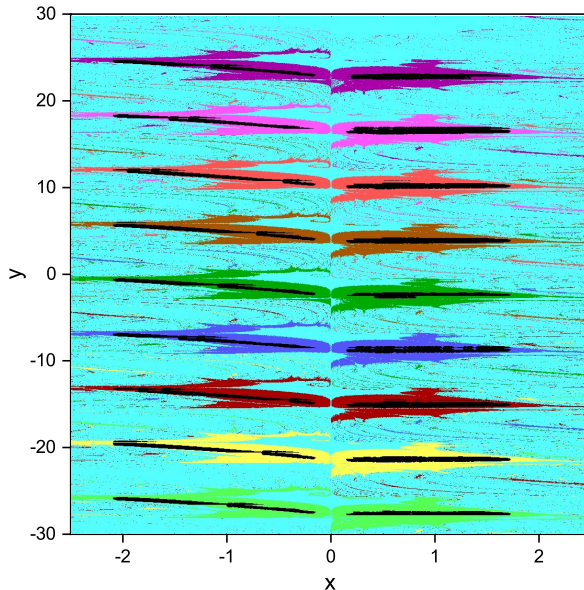
Fig. 3. (Colour online) Basins of attraction of the map (5) in the region $\{(x,y)|x \in [-2.5, 2.5], y \in [-30, 30]\}$. Unbounded basin of attraction which is the set of initial points going into in the region ($\{(x,y)||x| + |y| > 100\}$) is shown in cyan, the coexisting chaotic attractors are shown in black dots. The basin of chaotic attractors are shown in red, light red, blue, light blue, green, light green, brown, magenta and light megenta, respectively.

(b), respectively. From Fig. 4, the Lyapunov exponent diagram are consistent with the bifurcation diagram.

As can be seen from Fig. 4(a), when $a = 2.3$, the map (1) shows a period-2 solution. As a increases to 2.3825, there is a period-doubling bifurcation, and the period-2 solution bifurcates to a period-4 solution. When $a = 2.5078$, another period-doubling bifurcation is encountered, and this period-4 solution bifurcates to a period-8 solution. At $a = 2.5370$, this period-8 solution bifurcates to a period-16 solution, and then becomes chaos after a period-doubling cascade. For $a \in [2.6242, 2.6347]$, the map experiences a small window of period-6 and period-12 solutions, and bifurcates into chaos again at $a = 2.6350$ through a period-doubling cascade. Finally, when $a = 2.7150$, the two-piece chaotic attractors are jointed together into one-piece chaotic attractors.

Fig. 5 presents the phase portraits of the coexisting period-2 and period-6 solutions for the map (1) calculated at $(a, b, c) = (2.35, 1, 0.1)$ and $(a, b, c) = (2.625, 1, 0.1)$ in the region $\{(x,y)|x \in [-2, 2], y \in [-30, 30]\}$, respectively. Period-2 solutions of the map (1) were obtained by using the initial conditions $(1, -27)$, $(1, -20)$, $(1, -14)$, $(1, -8)$, $(1, -1)$, $(1, 5)$, $(1, 10)$, $(1, 17)$ and $(1, 24)$, and period-6 solutions were obtained by using $(1, -26)$, $(1, -20)$, $(1, -14)$, $(1, -7)$, $(1, -1)$, $(1, 5)$, $(1, 12)$, $(1, 18)$, and $(1, 24)$. From Fig. 5, we know that the coexisting periodic attractors have the same shape but at different positions. So it is a homogenous extreme multi-stability. For $a \in [2.29, 2.73]$ and other fixed parameters, the map has infinitely many coexisting attractors of different types including period-2 solutions, higher periodic solutions and chaotic attractors.

In order to show the complex dynamics of the map (1), bifurcation and Lyapunov exponent spectrum diagrams of the map were plotted in Fig. 6 by using a, b and c as branching parameters calculated for $(b, c) = (1, 0.1)$, $(a, c) = (2.7, 0.1)$ and $(a, b) = (2.7, 1)$, respectively, with the initial value chosen at $(1, -3)$. Comparing Fig. 4 (a)-(b) and Fig. 6 (a)-(b), the dynamics of the map (1) for $a \in [2.29, 2.73]$ is similar to that for $a \in [-2.7, -2.3]$. However, there is a reverse period-doubling cascade leading to chaos for $a \in [-2.7, -2.3]$. From Fig. 6 (c)-(d) and Fig. 6 (e)-(f), the map (1) is in chaotic regime and displays two-piece chaotic attractors
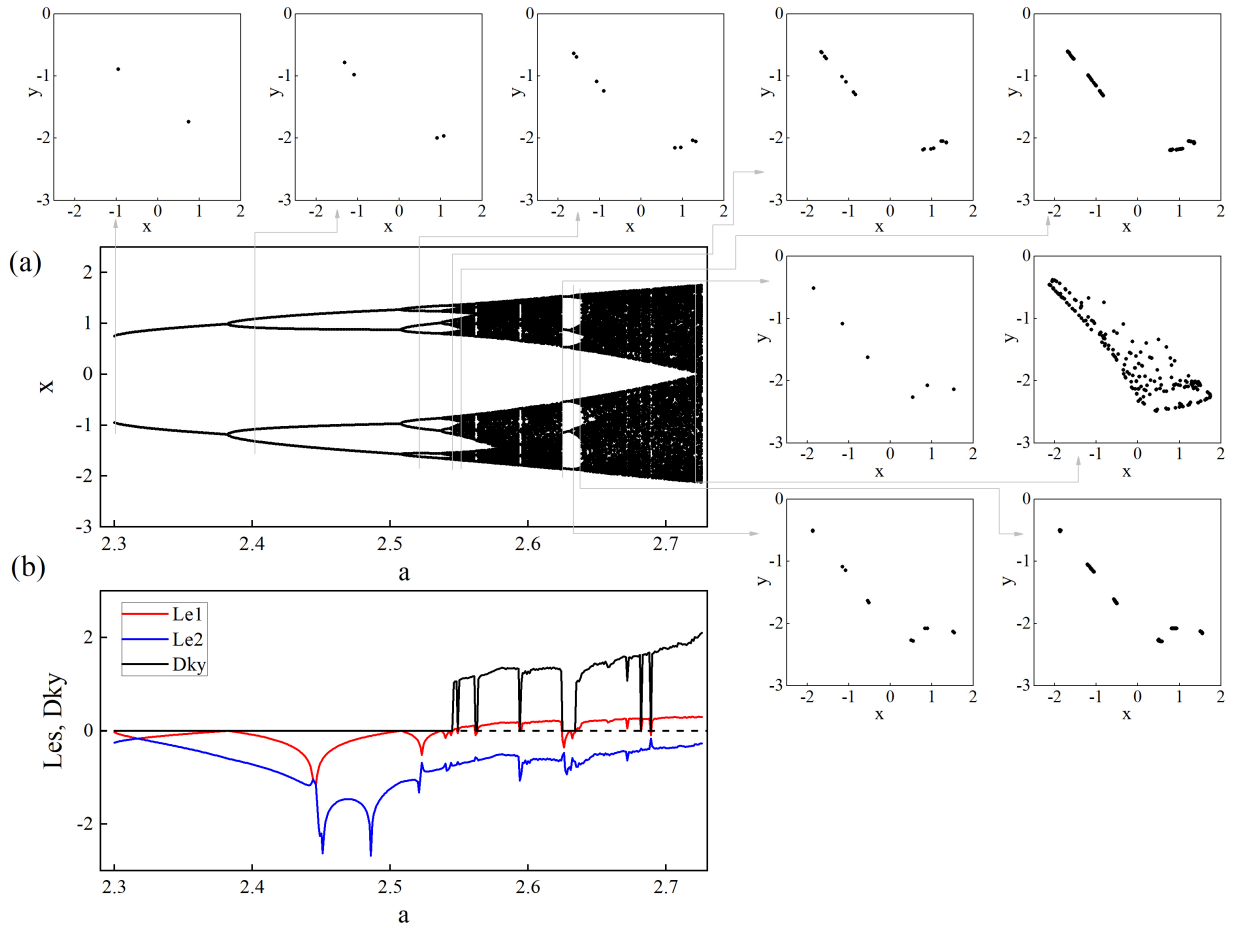
6

Fig. 4. (Colour online) Bifurcation diagrams of (a) x, and (b) Lyapunov exponent spectrum (LEs) and Lyapunov (Kaplan-Yorke) dimension (Dky) of the map (1) calculated for $a \in [2.29, 2.73]$ and $(b, c) = (1, 0.1)$ using the initial value $(1, -3)$.

In Fig. 4 (b), the largest Lyapunov exponent (Le1), the smallest Lyapunov exponent (Le2) and Lyapunov (Kaplan-Yorke) dimension (Dky) are indicated by red, blue and black lines, respectively. Additional windows demonstrate representative phase portraits of the map (1) calculated for $a = 2.300$ (period-2 solution), $a = 2.400$ (period-4 solution), $a = 2.522$ (period-8 solution), $a = 2.542$ (period-16 solution), $a = 2.550$ (five-piece chaotic solution), $a = 2.625$ (period-6 solution), $a = 2.634$ (period-12 solution), $a = 2.636$ (six-piece chaotic solution), and $a = 2.726$ (one-piece chaotic solution).
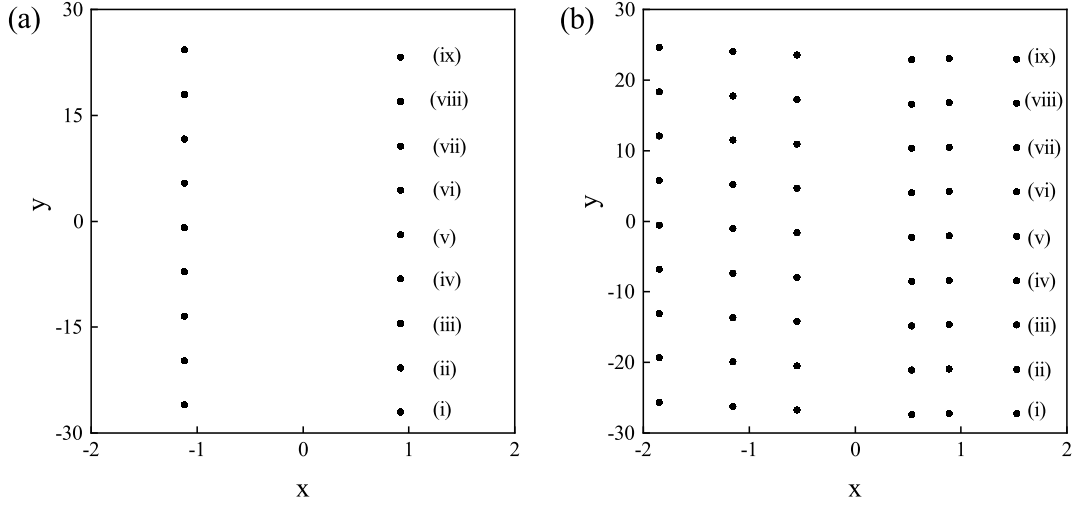
Fig. 5. Phase portraits of coexisting (a) period-2 and (b) period-6 solutions of the map (1) calculated at $(a, b, c) = (2.35, 1, 0.1)$ and $(a, b, c) = (2.625, 1, 0.1)$ in the region $\{(x, y) | x \in [-2, 2], y \in [-30, 30]\}$. Period-2 solutions of the map (1) were obtained for $x(0) = 1$ and (i) $y(0) = -27$, (ii) $y(0) = -20$, (iii) $y(0) = -14$, (iv) $y(0) = -8$, (v) $y(0) = -1$, (vi) $y(0) = 5$, (vii) $y(0) = 10$, (viii) $y(0) = 17$, (ix) $y(0) = 24$. Period-6 solutions of the map (1) were obtained for $x(0) = 1$ and (i) $y(0) = -26$, (ii) $y(0) = -20$, (iii) $y(0) = -14$, (iv) $y(0) = -7$, (v) $y(0) = -1$, (vi) $y(0) = 5$, (vii) $y(0) = 12$, (viii) $y(0) = 18$, (ix) $y(0) = 24$.
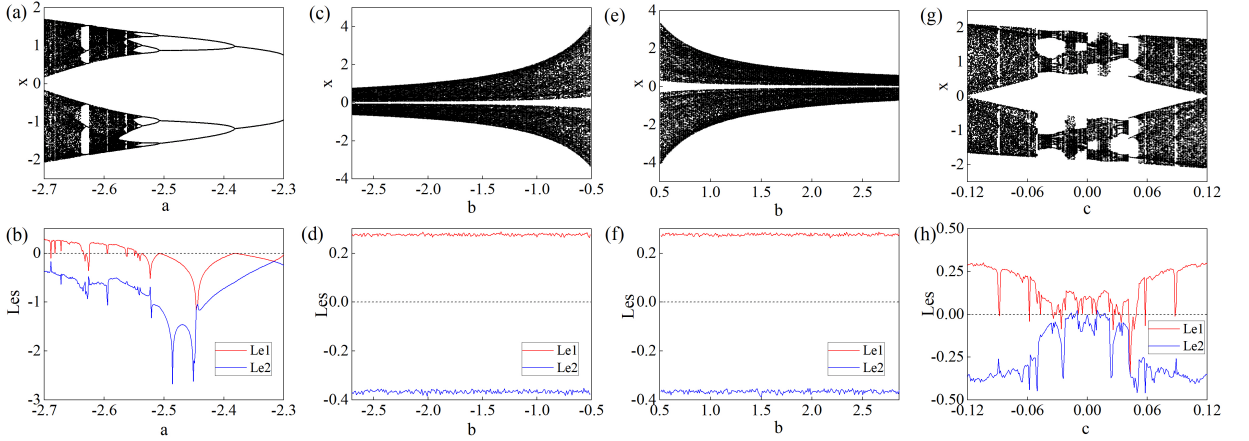

Fig. 6. (Colour online) Bifurcation diagrams of (a) x, and (b) Lyapunov exponent spectrum (LEs) of the map (1) calculated for $a \in [-2.7, -2.3]$ and $(b, c) = (1, 0.1)$. Bifurcation diagrams of (c) x, and (d) Lyapunov exponent spectrum (LEs) of the map (1) calculated for $b \in [-2.7, -0.5]$ and $(a, c) = (2.7, 0.1)$. Bifurcation diagrams of (e) x, and (f) Lyapunov exponent spectrum (LEs) of the map (1) calculated for $b \in [0.5, 2.7]$ and $(a, c) = (2.7, 0.1)$. Bifurcation diagrams of (g) x, and (h) Lyapunov exponent spectrum (LEs) of the map (1) calculated for $c \in [-0.12, 0.12]$ and $(a, b) = (2.7, 1)$. The initial values were all chosen at $(1, -3)$.

In Fig. 6 (b)(d)(f)(h), the largest Lyapunov exponent (Le1) and the smallest Lyapunov exponent (Le2) are indicated in red and blue lines, respectively.

for $b \in [-2.7, -0.5]$ and $b \in [0.5, 2.7]$. It should be noted that the absolute value of x becomes larger if b tends to infinity. When $b = 0$, the second equation of the map (1) becomes $y_{k+1} = y_k + c$. Since $a = 2.7 > 0$ and $c = 0.1 > 0$, the absolute value of x and the value of y tend to infinity. According to Fig. 6 (g), the map (1) exhibits complex dynamics including both chaotic and periodic solutions for $c \in [-0.12, 0.12]$, which can be confirmed from Fig. 6 (h).

4. Conclusions

Chaotic dynamics of a class of two-dimensional maps with homogenous extreme multi-stability was studied in this paper. A computer searching program was used to explore some simple chaotic maps by using phase portraits. Numerical methods, including computations of basins of attraction and the Lyapunov exponent spectrum, and bifurcation analysis, were used to demonstrate the complex dynamical behaviors of these maps. The maps also have infinitely many coexisting attractors in different types, such as coexisting periodic attractors and coexisting chaotic attractors. The coexisting attractors have the same shape but at different positions. The proposed chaotic maps can be used to generate chaotic signals for applications of chaos-based information engineering, such as data and image encryption [47]. Future works will focus on investigation of the high dimensional maps with infinitely many coexisting attractors and the construction of maps showing heterogeneous extreme multi-stability.

Acknowledgements

References

[1] Pisarchik A N and Feudel U 2014 *Phys. Rep.* **540** 167

[2] Li C B and Sprott J C 2013 *Int. J. Bifurc. Chaos* **23** 1350199

[3] Li C B and Sprott J C 2014 *Int. J. Bifurc. Chaos* **24**, 1450131

[4] Han X J, Xia F B, Zhang C, and Yu Y 2017 *Nonlin. Dyn.* **88** 2693

[5] Han X J, Zhang C, Yu Y, and Bi QS 2017 *Int. J. Bifurc. Chaos* **27** 1750051

[6] Liu Y and Páez Chávez J 2017 *Physica D* **348** 1

[7] Yadav K, Prasad A, and Shrimali M D 2018 *Phys. Lett. A* **382** 2127

[8] Liu Y and Páez Chávez J 2017 *Nonlin. Dyn.* **88** 1289

[9] Li C B and Sprott J C 2014 *Int. J. Bifurc. Chaos* **24** 1450034

[10] Li C B, Sprott J C, and Xing H 2016 *Phys. Lett. A* **380** 1172

[11] Chawanya T 1996 *Prog. Theor. Phys.* **95** 679

[12] Chawanya T 1997 *Physica D* **109** 201

[13] Sun H Y, Scott S K, and Showalter K 1999 *Phys. Rev. E* **60** 3876

[14] Ngonghala C N, Feudel U, and Showalter K 2011 *Phys. Rev. E* **83** 056206

[15] Hens C R, Banerjee R, Feudel U, and Dana S K 2012 *Phys. Rev. E* **85** 035202

[16] Sprott J C and Li C B 2014 *Phys. Rev. E* **89** 066901

[17] Patel M S, Patel U, Sen A, Sethia G C, Hens C, Dana S K, Feudel U, Showalter K, Ngonghala C N, and Amritkar R E 2014 *Phys. Rev. E* **89** 022918

[18] Bao B C, Xu Q, Bao H, and Chen M 2016 *Electron. Lett.* **52** 1008

[19] Bao B C, Bao H, Wang N, Chen M, and Xu Q 2017 *Chaos Solit. Fract.* **94** 102

[20] Chang H, Li Y X, Yuan F, and Chen G R 2019 *Int. J. Bifurc. Chaos* **29** 1950086

[21] Li Q, Hu S, Tang S, and Zeng G 2014 *Int. J. Circuit Theory Applications* **42** 1172

[22] Yuan F, Wang G, and Wang X 2016 *Chaos* **26** 073107

[23] Li C B, Thio W J C, Iu H H C, and Lu T A 2018 *IEEE Access* **6** 12945

[24] Yuan F, Deng Y, Li Y X, and Wang G Y 2019 *Nonlinear Dyn.* **96** 389

[25] Bao B C, Jiang T, and Wang G Y 2017 *Nonlin. Dyn.* **89** 1157

[26] Chen M, Sun M, Bao H, Hu Y, and Bao B C 2019 *IEEE Trans. Ind. Electron.* 67 2197

[27] Bao H, Chen M, Wu H G, and Bao B C 2019 *Sci. China Tech. Sci.* DOI: 10.1007/s11431-019-1450-6

[28] Zhang Y Z, Liu Z, Wu H G, Chen S Y, and Bao B C 2019 *Chaos Solit. Fract.* **127** 354

[29] Ye X L, Wang X Y, Gao S, Mou J, Wang Z S, and Yang F F 2020 *Nonlin. Dyn.* **99** 1489

[30] Li C B, Wang X, and Chen G R 2017 *Nonlin. Dyn.* **90** 1335

[31] Li C B, Sprott J C, Hu W, and Xu Y J 2017 *Int. J. Bifurc. Chaos* **27** 1750160

[32] Li C B and Sprott J C 2018 *Phys. Lett. A* **382** 581

[33] Tang Y X, Khalaf A J M , Rajagopal K, Pham V T, Jafari S, and Tian Y 2018 *Chin. Phys. B* **27** 040502

[34] Jafari S, Ahmadi A, Panahi S, and Rajagopal K 2018 *Chaos Solit. Fract.* **108** 182

[35] Jafari S, Ahmadi A, Khalaf A J M, Abdolmohammadi H R, Pham V T, and Alsaadi F E 2018 *AEÜ-Int. J. Electron. Commun.* **89** 131

[36] Lai Q, Kuate P D K, Liu F, and Iu H H C 2019 *IEEE Trans. Circuits Syst. II* DOI: 10.1109/TCSI-I.2019.2927371

[37] Zhang S, Zeng Y C, Li Z J, Wang M J, and Xiong L 2018 *Chaos* **28** 013113

[38] Zhang X and Li Z J 2019 *Int. J. Non-Linear Mech.* **111** 14

[39] Mira C, Gardini L, Barugola A, and Cathala J C 1996 *Chaotic dynamics in two-dimensional noninvertible maps* (Singapore: World Scientific)

[40] Jiang H B, Liu Y, Wei Z C, and Zhang L P 2016 *Nonlin. Dyn.* **85** 2719

[41] Jiang H B, Liu Y, Wei Z C, and Zhang L P 2016 *Int. J. Bifurc. Chaos* **26** 1650206

[42] Jiang H B, Liu Y, Wei Z C, and Zhang L P 2019 *Int. J. Bifurc. Chaos* **29** 1950094

[43] Huynh V V, Ouannas A, Wang X, Pham V T, Nguyen X Q, and Alsaadi F E 2019 *Entropy* **21** 279

[44] Ouannas A, Khennaoui A A, Bendoukha S, Vo T P, Pham V T, and Huynh V V 2018 *Appl. Sci.* **8** 2640

[45] Khennaoui A A, Ouannas A, Bendoukha S, Grassi G, Wang X, Pham V T, and Alsaadi F E 2019 *Adv. Differ. Equ.* **2019** 412

[46] Ouannas A, Wang X, Khennaoui A A, Bendoukha S, Pham V T, and Alsaadi F E 2018 *Entropy* **20** 720

[47] Liu Z Y, Xia T C, and Wang J B 2018 *Chin. Phys. B* **27** 030502

[48] Hua Z Y, Zhou B H, and Zhou Y C 2018 *IEEE Trans. Ind. Electron.* **66** 1273

[49] Hua Z Y, Zhou Y C, and Bao B C 2019 *IEEE Trans. Ind. Informat.* **16** 887

[50] Simpson D J W 2014 *Int. J. Bifurc. Chaos* **24** 1430018

[51] Simpson D J W and Tuffley C P 2017 *Int. J. Bifurc. Chaos* **27** 1730010

[52] Sprott J C 1993 *Strange attractors: creating patterns in chaos* (New York: M&T books)

[53] Sprott J C 2010 *Elegant chaos: algebraically simple chaotic flows* (Singapore: World Scientific) pp.24-30

[54] Wolf A, Swift J B, Swinney H L, and Vastano J A 1985 *Physica D* **16** 285